

Giant exciton oscillator strength and radiatively limited dephasing in two-dimensional platelets

Ali Naeem,¹ Francesco Masia,¹ Sotirios Christodoulou,² Iwan Moreels,² Paola Borri,^{1,3} and Wolfgang Langbein^{1,*}

¹*Cardiff University School of Physics and Astronomy, The Parade, Cardiff CF24 3AA, United Kingdom*

²*Istituto Italiano di Tecnologia, Via Morego 30, IT-16163 Genova, Italy*

³*Cardiff University School of Biosciences, Museum Avenue, Cardiff CF10 3AX, United Kingdom*

(Received 30 March 2014; revised manuscript received 23 February 2015; published 30 March 2015)

We measured the intrinsic ground-state exciton dephasing and population dynamics in colloidal quasi-two-dimensional (2D) CdSe nanoplatelets at low temperature (5–50 K) using transient resonant four-wave mixing in heterodyne detection. Our results indicate that below 20 K the exciton dephasing is lifetime limited, with the exciton population lifetime being as fast as 1 ps. This is consistent with an exciton lifetime given by a fast radiative decay due to the large in-plane coherence area of the exciton center-of-mass motion in these quasi-2D systems compared to spherical nanocrystals. The radiative rate in such 2D platelet systems can be controlled by the platelet area over orders of magnitude.

DOI: [10.1103/PhysRevB.91.121302](https://doi.org/10.1103/PhysRevB.91.121302)

PACS number(s): 78.67.Hc, 42.50.Md, 63.22.-m, 78.47.nj

The colloidal synthesis of quasi-two-dimensional (2D) semiconductor nanostructures has attracted much attention, owing to the simplicity, flexibility, and low cost compared to epitaxial growth techniques, and the wealth of interesting fundamental properties and applications of quantum wells (QWs) in, e.g., optoelectronics and photovoltaics. High-quality colloidal zinc-blende CdSe nanoplatelets (NPLs) having a thickness of 1–2 nm were recently reported [1–3], and exhibit absorption spectra well described by a QW-like electronic structure. Remarkably, the synthesized ensembles can have a monolayer thickness purity better than 95%, and the inhomogeneous broadening corresponds to only about 20% of the monolayer splitting, which is similar to optimized epitaxial quantum wells [4]. Furthermore, the thickness quantization energy of 0.5–1 eV is much larger than the bulk exciton binding energy of 15 meV [5], such that the excitons are close to the 2D limit, providing a fourfold binding energy increase. The binding energy is further enhanced [6] by the lower dielectric constant $\epsilon \sim 2$ in the NPL surrounding, and the reduced dielectric constant $\epsilon_\infty \sim 6$ of CdSe for energies above the longitudinal optic (LO) phonon energy of 26 meV compared to $\epsilon_s \sim 10$ below, resulting in predicted exciton binding energies [7] in the 100–300 meV range. A similar effect has been recently reported in monolayers of transition-metal dichalcogenides such as WS₂ [8].

Since the exciton oscillator strength increases with the exciton binding energy, we can expect a fast exciton radiative decay. Recent reports showed photoluminescence (PL) lifetimes decreasing with decreasing temperature, and lifetimes of 200–400 ps were measured at low temperatures [2,3,7], two orders of magnitude faster than in spherical CdSe nanocrystals. Recently, temperature- and magnetic-field-dependent measurements were interpreted with a three-level model similar to that used in spherical nanocrystals [9]. It is understood theoretically and reported experimentally in epitaxially grown QWs that QW excitons exhibit an oscillator strength which increases with increasing extension of the exciton in-plane center-of-mass (CM) motion wave function [10–13], the so-called coherence area. We therefore expect that the fundamental

bright NPL exciton (BX) has a short radiative lifetime, decreasing with increasing NPL area.

The radiative decay rate also sets a lower limit to the homogeneous linewidth of an optical transition. Recent PL measurements in single NPLs at low temperature showed linewidths of 0.5–1 meV [3,7]. These would correspond to a population lifetime in the 1 ps range, significantly shorter than the measured PL decay time. It is, however, known that single quantum dot PL linewidths are affected by fluctuations of the emission energy during long acquisition times (so-called spectral diffusion), hence the reported linewidths give an upper limit to the homogeneous linewidth. Furthermore, the PL decay of nonresonantly excited platelets does not provide a measurement of the BX lifetime but reflects the density dynamics mediated by phonon-scattering across all occupied exciton states, including higher CM quantized exciton states of lower oscillator strength, and spin-forbidden dark states. The measured PL decay times of 200–400 ps are thus an upper limit of the BX decay time. To quantify the giant oscillator strength effect in NPL it is therefore crucial to directly measure the intrinsic homogeneous linewidth and lifetime of the BX.

We previously demonstrated in epitaxial quantum wells [14,15], self-assembled quantum dots [16,17], and colloidal nanocrystals [18–20] that transient resonant four-wave mixing (FWM) can measure the intrinsic exciton dephasing time in inhomogeneously broadened ensembles unaffected by spectral diffusion. In the present Rapid Communication, we have used three-beam FWM to measure the intrinsic exciton dephasing and population dynamics in colloidal zinc-blende CdSe NPLs in the temperature range from 5 to 50 K.

The investigated NPLs have been synthesized according to the method reported in Ref. [2]. The resulting NPL have a room-temperature emission around 515 nm, and the x-ray diffraction reveals that they possess a zinc-blende crystal structure. More details are given in the Supplemental Material [21]. An optical and structural characterization of the investigated NPL ensemble is shown in Fig. 1. The synthesis typically yields NPLs with a room-temperature PL quantum efficiency of 50% and PL lifetimes in the nanosecond range, indicating that the nonradiative decay due to defects is slow. Transmission electron microscopy shows NPLs with lateral dimensions of $L_x = 30.8 \pm 2.6$ nm and $L_y = 7.1 \pm 0.9$ nm.

*langbeinww@cardiff.ac.uk

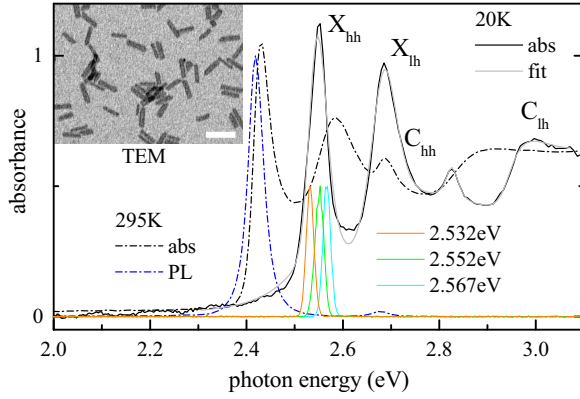


FIG. 1. (Color online) Linear optical properties of the investigated CdSe NPL ensemble. Absorption and photoluminescence spectra at 295 K (dashed-dotted lines), and absorption at 20 K with a fit (solid lines). The spectra of the laser pulses used in the FWM experiment are also shown, labeled according to their center photon energy. Inset: Transmission electron microscope (TEM) image of the NPLs. Scale bar: 50 nm.

Room-temperature absorption and emission spectra of the ensemble reveal a small Stokes shift (12 meV), and a wavelength of the lowest excitonic transition X_{hh} in absorption of 510 nm consistent with an electron/heavy-hole exciton confined in 6 (5) monolayer (ML) thickness according to Ref. [2] (Ref. [7]), respectively. The NPL surface is terminated by Cd [22], resulting in a half-integer ML thickness, so that we use 5.5 ML, $L_z = 1.67$ nm. At $T = 20$ K the absorption spectrum shifts to higher energies and exhibits a narrower X_{hh} due to the reduction of the phonon-scattering related homogenous broadening [3,7]. The absorption line shape at low temperature was fitted by a sum of two excitonic peaks X_{hh}, X_{lh} and continuum edges C_{hh}, C_{lh} , plus an additional peak for the 4.5 ML contribution (for details see the Supplemental Material). We inferred a X_{hh} linewidth of (46 ± 1) meV full width at half maximum (FWHM) dominated by inhomogeneous broadening. Furthermore, excitonic binding energies of $R_{hh} = (178 \pm 34)$ meV and $R_{lh} = (259 \pm 3)$ meV are inferred from the fit. R_{hh} is consistent with the range of 100–300 meV predicted in calculations [7]. The difference of R_{hh} and R_{lh} can be attributed to the different in-plane hole dispersions, as the 2D exciton binding energy is proportional to the in-plane reduced mass. Notably, the heavy hole quantized by the NPL thickness has in plane a light-hole mass $m_{lh} = 0.19m_e$, and the light hole has in plane a heavy-hole mass $m_{hh} = 0.67m_e$, as deduced from the Pidgeon-Brown model used in Ref. [2]. With the isotropic electron mass of $m_e = 0.18m_e$, this results in an in-plane reduced mass of $\mu_{hh} = 0.092m_e$ for X_{hh} and $\mu_{lh} = 0.14m_e$ for X_{lh} . The expected ratio of binding energies is thus $R_{lh}/R_{hh} = \mu_{lh}/\mu_{hh} = 1.51$, which is close to the ratio of 1.4 inferred from the fit.

Similar to previous works on CdSe nanocrystals [19,20], we have measured the dephasing time of the BX using transient three-beam FWM (see the sketch in Fig. 2) in resonance with X_{hh} (see the laser spectra in Fig. 1). All beams are derived from a train of 150 fs pulses with a 76 MHz repetition rate. The first pulse (P_1) induces a coherent polarization in the sample, which after a delay τ_{12} is converted

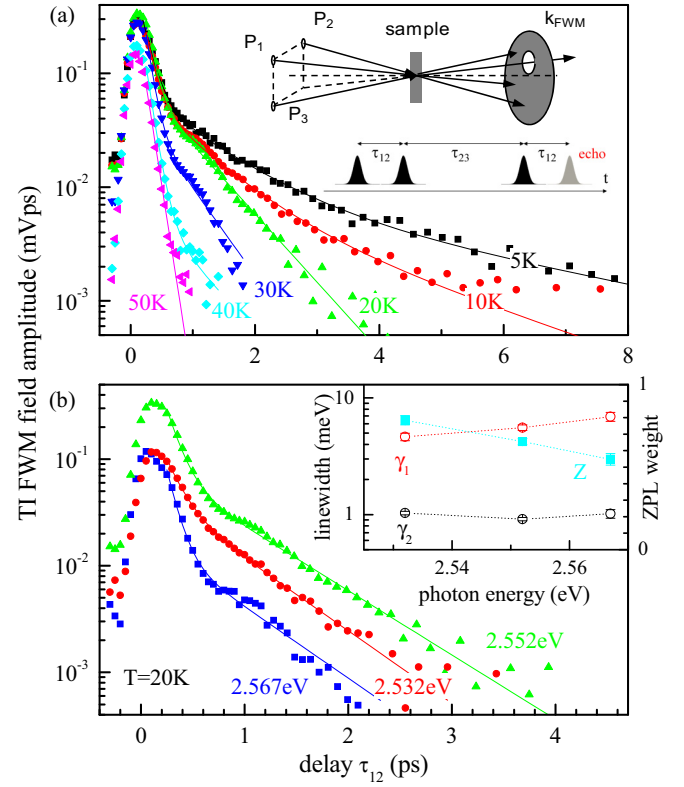


FIG. 2. (Color online) Time-integrated (TI) FWM field amplitude vs τ_{12} at $\tau_{23} = 1$ ps. The lines are fits to the data. (a) At different temperatures, as indicated, for a center energy of 2.552 eV. The inset shows a sketch of the pulse sequence and the directional selection. (b) For different center energies, as indicated (spectra given in Fig. 1), at a temperature of 20 K. The inset shows the resulting linewidths $2\hbar\gamma_{1,2}$.

into a density grating by the second pulse (P_2). The third pulse (P_3), delayed by τ_{23} from P_2 , is diffracted by this density grating, yielding the FWM signal. In the employed heterodyne technique [23] the pulse trains are radio-frequency shifted, resulting in a frequency-shifted FWM field which is detected by its interference with a reference pulse. In the investigated inhomogeneously broadened ensemble, the FWM signal is a photon echo emitted at a time τ_{12} after P_3 , and the microscopic dephasing is inferred from the decay of the photon-echo amplitude versus τ_{12} . Conversely, the decay of the photon-echo amplitude versus τ_{23} probes the exciton density dynamics [24].

The measured FWM field amplitude versus τ_{12} is given in Fig. 2 by the detected voltage (see the Supplemental Material). Measurements were taken at $\tau_{23} = 1$ ps to exclude nonresonant nonlinearities. The time-averaged excitation intensity was 17 W/cm² per beam, within the third-order nonlinear response regime and resulting in negligible local heating, as we affirmed by power-dependent measurements. To minimize selective excitation of linearly polarized transitions in the ensemble of randomly oriented NPLs, all pulses were co-circularly polarized. The decay of the FWM amplitude versus τ_{12} is described by two exponentially decaying components $\propto \exp(-2\gamma\tau_{12})$ for temperatures T above 10 K, with an additional longer component γ_3 visible for lower

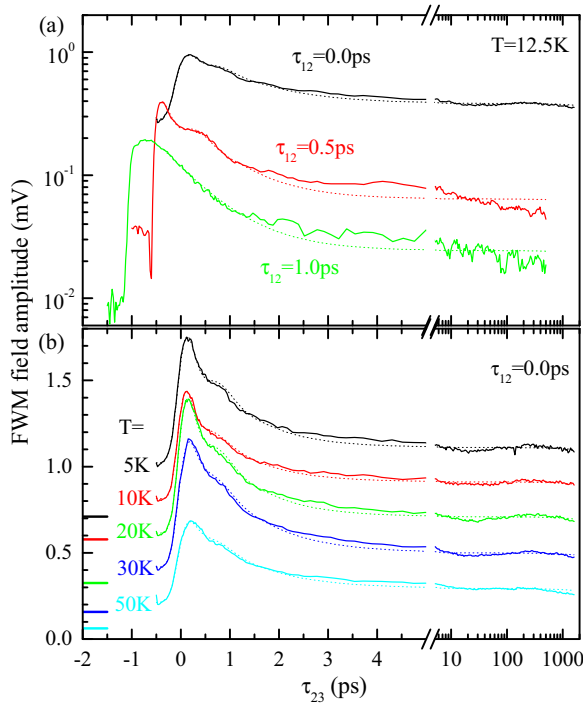


FIG. 3. (Color online) FWM field amplitude vs τ_{23} at fixed τ_{12} . Dashed lines are fits to the data. (a) For $T = 12.5$ K for different values of τ_{12} , as indicated. (b) For $\tau_{12} = 0$ ps for different temperatures, as indicated. The data are offset for clarity, as indicated by the bars.

temperatures, as shown by fits to the data for $\tau_{12} > 0.3$ ps. The dynamics is somewhat dependent on the probed energy within the inhomogeneously broadened ensemble, as shown in Fig. 2(b). The FWHM homogeneous linewidths $2\hbar\gamma$ of the fitted dephasing rates $\gamma_1 > \gamma_2$ (see the inset) show that γ_1 slightly increases with increasing energy across the inhomogeneous distribution, together with its relative weight [shown by the zero-phonon-line (ZPL) weight as discussed later], while γ_2 is slightly decreasing. All further experiments were done at 2.552 eV.

To investigate the physical origin of the observed dephasing, we have determined the exciton population dynamics by measuring FWM vs τ_{23} . The result for $\tau_{12} = 0$ shown in Fig. 3(b) can be described by two exponential decays with weakly temperature-dependent times around 1 ps and 40 ns. The latter is giving rise to a signal at $\tau_{23} < 0$ due to a pileup of the response from previous pulse repetitions of 13 ns period which excited the sample earlier. A damped oscillation with a period of about 1 ps is also observed, which is assigned to the modulation of the excitonic absorption by the coherent phonons created by the impulsive excitation, as has been previously observed in a variety of structures, including CdSe [25,26] and PbS [27] quantum dots (QDs). All data were fitted by the sum of two exponential decays including the pileup effect and the phonon oscillation, as discussed in detail in the Supplemental Material, yielding the decay rates $\Gamma_1 > \Gamma_2$ and amplitudes $A_{1,2}$.

Interestingly, when changing τ_{12} from 0 to 1 ps, A_1/A_2 increases, such that the relevance of the pileup effect decreases,

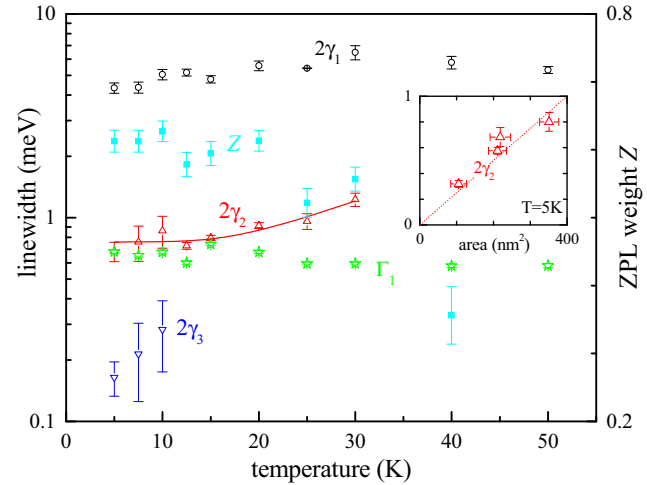


FIG. 4. (Color online) Homogeneous linewidths $2\hbar\gamma_{1,2,3}$, lifetime-limited linewidth $\hbar\Gamma_1$, and zero-phonon-line weight Z vs temperature. The line is a fit to the data for γ_2 . The inset shows the measured γ_2 at $T = 5$ K as a function of the NPL area.

while the rates are unchanged within error. This shows that the density-induced absorption of the A_2 component is spectrally broader than that of A_1 . A possible origin of the $\Gamma_2 \sim 25/\mu\text{s}$ component could be the spin-forbidden dark excitonic state. However, since we find that Γ_2 is nearly temperature independent from 5 to 50 K, we can estimate the related dark-bright splitting $\delta_0 > k_B T \log(\Gamma_2/\Gamma_1) \sim 40$ meV for $T = 50$ K. This is much larger than the 1–10 meV found in colloidal CdSe QDs. We also do not find evidence for an internal relaxation between different bright/dark excitonic states, which modifies the dynamics for $\tau_{12} \neq 0$ as observed on spherical nanocrystals [19,20]. A more likely interpretation is charging of the NPL by carrier trapping in the surrounding, leaving a long-lived remaining carrier, which is also consistent with the spectral broadening of the response.

The FWHM linewidth $\hbar\Gamma_1$ due to the density decay and the homogeneous widths $2\hbar\gamma_{1,2}$ are shown in Fig. 4 as a function of temperature. Remarkably, $2\gamma_2$ is equal to Γ_1 within error for $T \lesssim 10$ K. We therefore attribute γ_2 to the zero-phonon-line (ZPL) dephasing of the BX transition in NPLs, which is lifetime limited at low temperature. The deduced low-temperature ZPL width of $2\hbar\gamma_0 = 0.7$ meV is consistent with PL linewidths measured on individual NPLs at low temperature [3,7], and about two orders of magnitude larger than in spherical QDs, where coherence times of up to 100 ps, corresponding to 6 μeV linewidths, have been measured [19,20]. The temperature dependence of γ_2 shown in Fig. 4 is fitted by a temperature-activated behavior $2\hbar\gamma_2 = 2\hbar\gamma_0 + b/[\exp(\Delta/k_B T) - 1]$, yielding a spontaneous scattering rate $b = 6$ meV and an activation energy $\Delta = 7 \pm 3$ meV. The line narrowing in the X_{hh} absorption from room temperature to low temperature seen in Fig. 1 is consistent with these values. To discuss the scattering process leading to the dephasing, we have estimated the energy separation between the BX state and the first excited state from the quantization of the exciton CM motion. We use the “exciton-in-a-box” quantization energy

$\frac{\hbar^2 \pi^2}{2M} \left(\frac{n_x^2}{(L_x - 2a_B)^2} + \frac{n_y^2}{(L_y - 2a_B)^2} \right)$, where $n_{x,y} = 1, 2, \dots$ are the quantum numbers, a_B is the in-plane exciton Bohr radius of about 2 nm, and $M = 0.37m_e$ is the exciton CM mass, given by the sum of electron and hole mass from the Pidgeon-Brown model. The resulting energy separation of the BX $(n_x, n_y) = (1, 1)$ to the first excited state $(2, 1)$ is 4 meV, which is similar to Δ . The temperature dependence of γ_2 could thus be related to scattering into the $(2, 1)$ state by acoustic phonon absorption. Note that the $(2, 1)$ state has an odd parity and is thus dark.

The weak longer dephasing component γ_3 of amplitude A_3 observable for $T \leq 10$ K in Fig. 2 is attributed to a fraction of NPLs in the ensemble with significant exciton in-plane localization, reducing the coherence area and thus the radiative rate. This is compatible with the density dynamics shown in Fig. 3, since the small (13%) fraction of NPLs as given by relative amplitude $A_3/(A_3 + A_2)$ is not easily appreciable. However, suppressing the long-lived Γ_2 component [see $\tau_{12} = 1$ ps in Fig. 3(a)], a weak component with a decay time of about 5 ps is observed, which is consistent with the dephasing-limited lifetime $1/(2\gamma_3) \sim 5$ ps.

The dephasing rate γ_1 has a relative amplitude which increases with increasing temperature, indicating that this fast initial dephasing is due to phonon-assisted transitions. Excitons confined in quantum dots exhibit a non-Lorentzian homogeneous line shape, consisting of a sharp zero-phonon line superimposed onto a few meV wide acoustic phonon band, which in turn gives rise to an initial fast dephasing [17,19]. Since excitons in the investigated NPLs are confined in a larger volume ($\sim 500 \text{ nm}^3$) than in the nanocrystals studied in Ref. [19] ($\sim 200 \text{ nm}^3$), we expect a higher ZPL weight Z . We determine Z from the initial amplitude decay, as discussed in the Supplemental Material. However, as shown in Fig. 4, we find values of $Z \sim 0.6$ at low temperature, which is similar to the values found in spherical nanocrystals [19]. The smaller than expected value of Z is attributed to an enhancement of the phonon-assisted transitions by the available excited exciton states on the high energy side of the ZPL, forming exciton-polaron transitions [28]. This attribution is consistent with the observed decrease of Z with increasing energy within the X_{hh} absorption line [see Fig. 2(b)]. Interestingly, single NPL spectra at $T = 20$ K [3] show an emission peak with a satellite shifted by about 4 meV to higher energies having a relative weight of about 10%. Considering that the Boltzmann factor of thermal population for 4 meV separation is about 0.1, we can estimate that this satellite has a similar absorption as the main peak, consistent with the ZPL weight of $Z = 0.6$ deduced from the FWM dynamics.

Let us now discuss the physical interpretation of the most important finding, the measured exciton lifetime of about 1 ps. When compared to the ~ 10 ns radiative lifetime in CdSe spherical nanocrystals [29], this lifetime is remarkably short. It is known that with increasing exciton CM extension the radiative lifetime decreases [10,11], an effect also referred to as “giant oscillator strength” [7,10]. The radiative lifetime of a heavy-hole exciton has been calculated to be 12 ps in a 10 nm wide GaAs/AlGaAs QW [30], and measured to be about 1 ps in 10 nm wide ZnSe/ZnMgSSe QWs [31] and 16–20 nm wide ZnSe/ZnMgSe QWs [32]. Considering the large exciton binding energy $R_{hh} \sim 180$ meV compared to the ZnSe QWs which have an exciton binding energy ~ 25 meV, we expect a free exciton radiative lifetime in extended NPLs in the order of 100 fs. The measured lifetime of ~ 1 ps is thus consistent with excitons being localized in plane by the lateral size of the NPLs, whereby the lifetime increases due to the reduced coherence area [13]. For NPL much smaller than the wavelength and much larger than a_B , the radiative rate is expected to be proportional to the NPL area. The measured low-temperature $2\hbar\gamma_2$ for NPLs of different sizes ($24 \times 5, 27 \times 8, 31 \times 7, 27 \times 13$) nm² is given in the inset of Fig. 4. We find within error a proportionality to the NPL area, as expected for radiative decay.

In conclusion, we have presented evidence of an intrinsic radiative lifetime in the 1 ps range in quasi-2D CdSe nanoplatelets from dephasing and density dynamics measured by three-beam four-wave mixing. The radiative rate is scaling with the exciton coherence area, promising a tuning range from hundreds of picoseconds down to subpicoseconds adjusting the platelet area, and merging the size tunability and monolayer thickness precision of colloidal synthesis with the large oscillator strength of quantum well excitons. These nanoplatelets are expected to enable strong light-matter coupling in tunable microcavities [33], and applications as single photon switches.

A.N. acknowledges financial support by the President’s Research Scholarship program of Cardiff University. A.N. and F.M. acknowledge financial support from the UK EPSRC Research Council (Grants No. EP/H45848/1 and No. EP/I016260/1) and from the European Union (Marie Curie Grant Agreement No. PERG08-GA-2010-276807). P.B. acknowledges the UK EPSRC Research Council for support from a Leadership fellowship award (Grant No. EP/I005072/1). W.L. acknowledges support from a Leverhulme Royal Society Research Fellowship (Grant No. LT20085). The authors thank Roberta Ruffilli for the preparation and measurement of the cross-section TEM samples.

-
- [1] S. Ithurria and B. Dubertret, *J. Am. Chem. Soc.* **130**, 16504 (2008).
 [2] S. Ithurria, M. D. Tessier, B. Mahler, R. P. S. M. Lobo, B. Dubertret, and A. L. Efros, *Nat. Mater.* **10**, 936 (2011).
 [3] M. D. Tessier, C. Javaux, I. Maksimovic, V. Lorient, and B. Dubertret, *ACS Nano* **6**, 6751 (2012).

- [4] K. Leosson, J. R. Jensen, W. Langbein, and J. M. Hvam, *Phys. Rev. B* **61**, 10322 (2000).
 [5] J. Voigt, F. Spiegelberg, and M. Senoner, *Physica Status Solidi B* **91**, 189 (1979).
 [6] E. A. Muljarov, S. G. Tikhodeev, N. A. Gippius, and T. Ishihara, *Phys. Rev. B* **51**, 14370 (1995).

- [7] A. Achtstein, A. Schliwa, A. Prudnikau, M. Hardzei, M. Artemyev, C. Thomsen, and U. Woggon, *Nano Lett.* **12**, 3151 (2012).
- [8] A. Chernikov, T. C. Berkelbach, H. M. Hill, A. Rigosi, Y. Li, O. B. Aslan, D. R. Reichman, M. S. Hybertsen, and T. F. Heinz, *Phys. Rev. Lett.* **113**, 076802 (2014).
- [9] L. Biadala, F. Liu, M. D. Tessier, D. R. Yakovlev, B. Dubertret, and M. Bayer, *Nano Lett.* **14**, 1134 (2014).
- [10] J. Feldmann, G. Peter, E. O. Göbel, P. Dawson, K. Moore, C. Foxon, and R. J. Elliott, *Phys. Rev. Lett.* **59**, 2337 (1987).
- [11] L. C. Andreani, G. Panzarini, and J.-M. Gérard, *Phys. Rev. B* **60**, 13276 (1999).
- [12] J. Hours, P. Senellart, E. Peter, A. Cavanna, and J. Bloch, *Phys. Rev. B* **71**, 161306(R) (2005).
- [13] V. Savona and W. Langbein, *Phys. Rev. B* **74**, 075311 (2006).
- [14] P. Borri, W. Langbein, J. M. Hvam, and F. Martelli, *Phys. Rev. B* **60**, 4505 (1999).
- [15] W. Langbein and J. M. Hvam, *Phys. Rev. B* **61**, 1692 (2000).
- [16] P. Borri, W. Langbein, S. Schneider, U. Woggon, R. L. Sellin, D. Ouyang, and D. Bimberg, *Phys. Rev. Lett.* **87**, 157401 (2001).
- [17] P. Borri, W. Langbein, U. Woggon, V. Stavarache, D. Reuter, and A. D. Wieck, *Phys. Rev. B* **71**, 115328 (2005).
- [18] F. Masia, W. Langbein, I. Moreels, Z. Hens, and P. Borri, *Phys. Rev. B* **83**, 201309(R) (2011).
- [19] F. Masia, N. Accanto, W. Langbein, and P. Borri, *Phys. Rev. Lett.* **108**, 087401 (2012).
- [20] N. Accanto, F. Masia, I. Moreels, Z. Hens, W. Langbein, and P. Borri, *ACS Nano* **6**, 5227 (2012).
- [21] See Supplemental Material at <http://link.aps.org/supplemental/10.1103/PhysRevB.91.121302> for more details on several topics, which also includes Refs. [34–57].
- [22] I. Fedin and D. V. Talapin, *J. Am. Chem. Soc.* **136**, 11228 (2014).
- [23] P. Borri and W. Langbein, in *Semiconductor Quantum Bits*, edited by O. Benson and F. Henneberger (World Scientific, Singapore, 2009).
- [24] J. Shah, *Ultrafast Spectroscopy of Semiconductors and Semiconductor Nanostructures* (Springer, Berlin, 1996), Chap. 2.
- [25] D. M. Mittleman, R. W. Schoenlein, J. J. Shiang, V. L. Colvin, A. P. Alivisatos, and C. V. Shank, *Phys. Rev. B* **49**, 14435 (1994).
- [26] L. Dworak, V. V. Matylitsky, M. Braun, and J. Wachtveitl, *Phys. Rev. Lett.* **107**, 247401 (2011).
- [27] T. D. Krauss and F. W. Wise, *Phys. Rev. Lett.* **79**, 5102 (1997).
- [28] V. N. Gladilin, S. N. Klimin, V. M. Fomin, and J. T. Devreese, *Phys. Rev. B* **69**, 155325 (2004).
- [29] S. A. Crooker, T. Barrick, J. A. Hollingsworth, and V. I. Klimov, *Appl. Phys. Lett.* **82**, 2793 (2003).
- [30] L. C. Andreani, *Confined Electrons and Photons: New Physics and Applications* (Plenum, New York, 1995), pp. 57–112.
- [31] W. Langbein, C. Mann, U. Woggon, M. Klude, and D. Hommel, *Phys. Status Solidi A* **190**, 861 (2002).
- [32] H. P. Wagner, A. Schätz, R. Maier, W. Langbein, and J. M. Hvam, *Phys. Rev. B* **57**, 1791 (1998).
- [33] P. R. Dolan, G. M. Hughes, F. Grazioso, B. R. Patton, and J. M. Smith, *Opt. Lett.* **35**, 3556 (2010).
- [34] M. D. Tessier, L. Biadala, C. Bouet, S. Ithurria, B. Abecassis, and B. Dubertret, *ACS Nano* **7**, 3332 (2013).
- [35] R. F. Schnabel, R. Zimmermann, D. Bimberg, H. Nickel, R. Lösch, and W. Schlapp, *Phys. Rev. B* **46**, 9873 (1992).
- [36] A. Pasquarello and L. C. Andreani, *Phys. Rev. B* **44**, 3162 (1991).
- [37] W. Langbein, J. M. Hvam, and R. Zimmermann, *Phys. Rev. Lett.* **82**, 1040 (1999).
- [38] G. Kocherscheidt, W. Langbein, G. Mannarini, and R. Zimmermann, *Phys. Rev. B* **66**, 161314(R) (2002).
- [39] D. Gammon, E. S. Snow, B. V. Shanabrook, D. S. Katzer, and D. Park, *Science* **273**, 87 (1996).
- [40] M. Bayer and A. Forchel, *Phys. Rev. B* **65**, 041308(R) (2002).
- [41] A. Müller, E. B. Flagg, P. Bianucci, X. Y. Wang, D. G. Deppe, W. Ma, J. Zhang, G. J. Salamo, M. Xiao, and C. K. Shih, *Phys. Rev. Lett.* **99**, 187402 (2007).
- [42] W. Demtröder, *Laser Spectroscopy* (Springer, Berlin, 1998).
- [43] Y. R. Shen, *The Principles of Nonlinear Optics* (Wiley-Interscience, New York, 1984).
- [44] S. Mukamel, *Principles of Nonlinear Optical Spectroscopy* (Oxford University Press, New York, 1999).
- [45] S. T. Cundiff, *Opt. Express* **16**, 4639 (2008).
- [46] W. Langbein, *Riv. Nuovo Cimento Soc. Ital. Fis.* **33**, 255 (2010).
- [47] A. E. Siegman, *Lasers* (Oxford University Press, New York, 1986).
- [48] W. Langbein, P. Borri, U. Woggon, V. Stavarache, D. Reuter, and A. D. Wieck, *Phys. Rev. B* **69**, 161301(R) (2004).
- [49] V. Cesari, W. Langbein, and P. Borri, *Appl. Phys. Lett.* **94**, 041110 (2009).
- [50] W. Langbein, V. Cesari, F. Masia, A. B. Krysa, P. Borri, and P. M. Smowton, *Appl. Phys. Lett.* **97**, 211103 (2010).
- [51] P. Borri, V. Cesari, and W. Langbein, *Phys. Rev. B* **82**, 115326 (2010).
- [52] V. Cesari, W. Langbein, and P. Borri, *Phys. Rev. B* **82**, 195314 (2010).
- [53] F. Masia, W. Langbein, and P. Borri, *Appl. Phys. Lett.* **93**, 021114 (2008).
- [54] F. Masia, W. Langbein, P. Watson, and P. Borri, *Opt. Lett.* **34**, 1816 (2009).
- [55] F. Masia, W. Langbein, and P. Borri, *Phys. Rev. B* **85**, 235403 (2012).
- [56] F. Masia, W. Langbein, and P. Borri, *Phys. Chem. Chem. Phys.* **15**, 4226 (2013).
- [57] *Handbook on Physical Properties of Semiconductors*, edited by S. Adachi (Kluwer Academic, Dordrecht, 2004), Vol. 3.